Measurement of the Thermal Diffusivity of HTS (a mixture of molten $NaNO_3$–KNO_3–$NaNO_2$; 7–44–49 mole %) by Optical Interferometry

Osamu Odawara, Isao Okada, and Kazutaka Kawamura*
Research Laboratory for Nuclear Reactors, Tokyo Institute of Technology, O-okayama, Meguro-ku, Tokyo, Japan

The thermal diffusivity of HTS (heat transfer salt; $NaNO_3$–KNO_3–$NaNO_2$; 7–44–49 mole %) is measured over a wide range of temperatures by means of wave-front-shearing interferometry. The thermal conductivity K is calculated from this result and the existing data on the density and the specific heat and found to be expressed by $K = 0.519 - 4.7 \times 10^{-5}(T - 142)$ (160–420 °C). The temperature dependence of K in the present study is smaller than that in previous studies (ca. -5×10^{-4} W m^{-1} deg^{-2}). In order to check the reliability of the present method at high temperatures the thermal diffusivity of molten $NaNO_3$ is also measured; molten $NaNO_3$ is one of the salts whose data on the thermal diffusivity and the relating properties are widely available.

Measurement of thermal conductivity of liquids is much more difficult at elevated temperatures than at room temperature because of corrosion of cell materials, convection of liquids, and so on. Reliable data on thermal conductivity of molten salts are therefore limited. Gustafsson et al. (*6*) have applied wave-front-shearing interferometry, which was originally devised by Bryngdahl (*2*), to the measurement of thermal diffusivity of some molten salts below 500 °C by using "light ports" which connect the cell placed at elevated temperatures with the optical system placed at room temperature without disturbing the optical path of the light. It seems that this method is more reliable than other methods using thermocouples, such as "concentric cylinder methods" (*1*) and "hot wire methods" (*14*), since in this method only a very small rise in temperature is needed for the heat source (say, 0.2 °C) and the effect of convection can be removed from the calculation of thermal diffusivity.

The heat transferring material HTS is useful since it is stable over a relatively wide range of temperatures (200–600 °C) and its heat transfer coefficient is large (*15*). Reliable thermal data for this material are therefore indispensable for practical purposes. In the present study the thermal diffusivity of HTS is measured over a wide range of temperatures by means of wave-front-shearing interferometry and the thermal conductivity is calculated from the existing data on the density and the specific heat. In order to check this method with an interferometer set up in our laboratory, the thermal diffusivities of distilled water and molten $NaNO_3$ were first measured; data on the thermal diffusivity of distilled water and molten $NaNO_3$ measured with various methods by various investigators are available.

Experimental Section

The theory of wave-front-shearing interferometry (*2*) and its application to the measurement of thermal diffusivity of molten salts (*6*) have already been described in detail.

The optical system of the wave-front-shearing interferometer constructed in our laboratory was similar to that employed for the measurement of thermal diffusivity of some molten salts by Gustafsson (*6*). A 15-mW He–Ne gas laser was used as a light source. The cell was a stainless steel cylinder with an internal diameter of 90 mm and a height of 150 mm. Two slits of 20 mm in width and 10 mm in height, through which the light was to pass, were made at both sides of the cell wall. Two quartz windows, each with a diameter of 35 mm and a thickness of 10 mm, were attached tightly to the wall of the cell by aluminum holders to cover the slits from the outside and to keep a liquid inside the cell. The flatness of the windows was less than $\lambda/5$ and the parallelism of both surfaces was less than 2 seconds of arc. In experiments at elevated temperatures the cell was placed inside an electric furnace with a large heat capacity and a salt was melted in the cell. Then, an apparatus (see Figure 1) supporting a heat source was inserted into the liquid in the cell, and placed in such a way that the plane of heat source should be parallel to the direction of the light. The heat source was made of a silver foil whose approximate dimension was 85 mm in length, 20 mm in width, and 0.006 mm in thickness. Both the upper and lower ends of the foil were rolled round small silver rods, which were in turn connected to the copper support by screws. Two Pyrex-glass cylinders were pressed to the foil, the position of these being adjusted with stainless steel wires so that the foil was parallel to the copper support. The copper support had been electroplated with a thick layer (~20 μm) of silver in order to be free from corrosion. The upper silver plate was strained upward by a force of a spring. An alkaline storage battery of 2.4 V with a very small internal resistance was used as a power supply for the heating foil. First, distilled water was used as a testing material. Then, thermal diffusivities of molten $NaNO_3$ and HTS were measured. According to the method proposed by Gustafsson (*6*), in high temperature experiments two tubes called "light ports", the insides of which were evacuated to about 1 mmHg, were inserted through the wall of the electric furnace; these light ports enabled the light to travel straight in spite of the temperature gradient between the inside and the outside of the furnace. The switch which started the supply of electric current to the foil was synchronized with the shutter for the first exposure of the film. Interferograms were taken at intervals of 0.5 s over the period of about 15 s. The electric current and the voltage drop across the foil were recorded with an X-Y recorder.

HTS was prepared by weighing accurately and mixing the three salts ($NaNO_3$, KNO_3, $NaNO_2$), which had been fully dried. The ratio of the constituent cations, Na^+, and K^+ was checked by flame spectrophotometry and that of NO_2^- by iodometric titration.

The volume of the liquids needed for an experiment of the measurement of thermal diffusivity was about 700 mL.

Results

In the interferograms, a pair of dark fringes successively appeared at both sides of the foil images and spread outward with the elapse of time. If we designate the distances between a pair of fringes as X_1, X_2, X_3, . . . in ascending order of magnitude, it follows theoretically that $(X_i/\sqrt{\kappa t})$ should be constant before the onset of convection and that

$$\mathrm{erfc}(X_1/4\sqrt{\kappa t}) - \mathrm{erfc}(X_2/4\sqrt{\kappa t}) = \mathrm{erfc}(X_2/4\sqrt{\kappa t}) - \mathrm{erfc}(X_3/4\sqrt{\kappa t}) = \ldots \quad (1)$$

where $\mathrm{erfc}(s) = (2/\sqrt{\pi}) \int_s^\infty \exp(-\xi^2)\, d\xi = 1 - \mathrm{erf}(s)$ (*5*). Thus, from successive interferograms, κ can be calculated on the basis of at least three consecutive pairs of fringes using eq 1. For a typical experiment of HTS, X_i^2 is plotted against t in Figure 2.

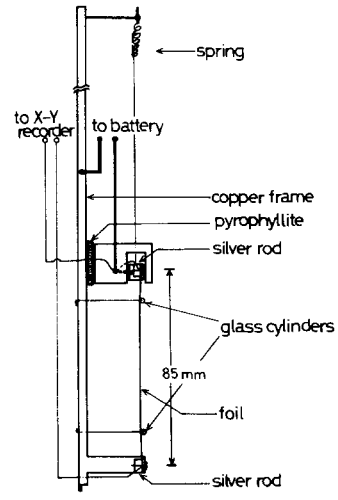

Figure 1. Arrangement for the support of the foil.

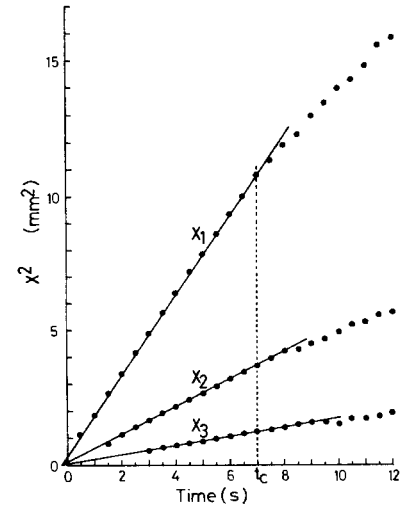

Figure 2. Plots of X^2 as a function of time for a typical experiment in HTS (168 °C).

Table I. Experimental Results Obtained from Measurement on Distilled Water

Temp (°C)	Thermal diffusivity $\times 10^7$ (m^2 s^{-1})	Onset of convection(s) Exptl	Calcd	Recommended values[a] $\times 10^7$ (m^2 s^{-1})
18.0	1.409	12	13	1.41_2
18.0	1.407	12	14	
18.5	1.411	15	15	1.41_4
18.5	1.417	16	17	
22.5	1.432	12	14	1.43_5
23.3	1.442	14	15	
23.3	1.447	14	16	1.44_0
23.3	1.444	15	16	
27.2	1.469	15	16	1.46_4
27.2	1.479	15	17	

[a] Literature values taken from TPRC Data (*13*).

Table II. Experimental Data for Molten $NaNO_3$

Temp (°C)	Power Qd (W m^{-1})	Thermal diffusivity $\times 10^7$ (m^2 s^{-1})	Thermal conductivity (W m^{-1} deg^{-1}) From eq 2[a]	From eq 3[b]
308	36.59	1.65	0.568	0.567
310	38.31	1.69	0.588	0.580
343	36.38	1.70	0.552	0.576
351	36.51	1.70	0.565	0.575
371	24.70	1.70	0.567	0.570
380	38.07	1.69	0.572	0.565
390	29.77	1.67	0.562	0.555
417	40.94	1.68	0.580	0.553
418	43.53	1.68	0.582	0.553

[a] Calculated with $(\partial n/\partial T) = -1.4232 \times 10^{-4}$ (*7*). [b] Calculated with C_p = 0.429 cal g^{-1} deg^{-1} and $\rho = 2.32 - 7.15 \times 10^{-4}$ $(T + 273)$ g cm^{-3} (*8*).

As seen from Figure 2, X_i^2 varies linearly with t until the convection occurs.

With a least-squares fit for the linear part of the line, X_i^2/t was calculated and the value of κ was determined.

The thermal diffusivity of distilled water determined in the present study is compared with the recommended value in Table I. This indicates that the present method is reliable at least at room temperature.

Since the refractive index of liquids n can be determined independently by means of wave-front-shearing interferometry (*16*), the thermal conductivity is calculated from the temperature dependence of the refractive index $(\partial n/\partial T)$

$$K = bQd(\partial n/\partial T)\{\mathrm{erfc}(X_2/4\sqrt{\kappa t}) - \mathrm{erfc}(X_1/4\sqrt{\kappa t})\}/\lambda \quad (2)$$

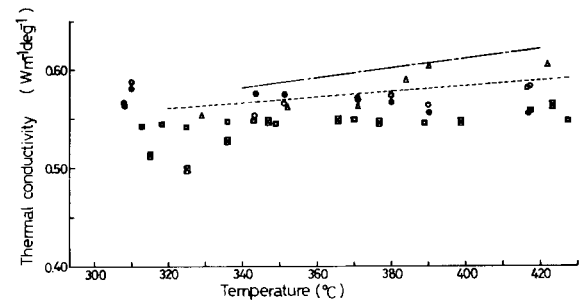

Figure 3. Thermal conductivity of molten $NaNO_3$: O, present results calculated from eq 2; ●, present results calculated from eq 3; △, Bloom et al. (*1*) (a concentric cylinder method); □, McLaughlin (*12*) (a hot wire method); ⊠, Gustafsson et al. (*6*) (an optical interferometric method; they have calculated these values from their thermal diffusivity data by using eq 2.); - - - -, White et al. (*17*) (a concentric cylinder method); - - - - -, McDonald (*11*) (a concentric cylinder method).

Alternatively, K can be calculated from the density and the specific heat by

$$K = \kappa C_p \rho \quad (3)$$

For molten $NaNO_3$, the thermal diffusivity and the thermal conductivity calculated by eq 2 (*7*) and 3 (*8*) are tabulated in Table II. The thermal conductivity is compared with those previously determined in Figure 3.

The thermal diffusivity of HTS is given in Table III. Since $(\partial n/\partial T)$ has not been determined for HTS, the thermal conductivity is calculated from the thermal diffusivity with the aid of eq 3 (*10*). This is tabulated in Table III and compared with those so far determined in Figure 4.

Discussion

Since the thermal diffusivity of distilled water measured in the present study is consistent with the recommended value within experimental error, the optical system of this interferometer is considered reliable.

A rise in the temperature at the heating foil during experiments is estimated roughly from the number of pairs of fringes m, using eq 4:

$$\Delta T = \Delta n/(\partial n/\partial T) = \Delta R/l\cdot(\partial n/\partial T) \simeq -m\lambda/l\cdot(\partial n/\partial T) \quad (4)$$

For example, in the case of molten $NaNO_3$, substituting $m = 4$, λ 632.8 nm, $l = 9$ cm, and $(\partial n/\partial T) = -1.4 \times 10^{-4}$ into eq 4 yields $\Delta T \simeq 0.2$ °C; thus, the rise in temperature is very small as compared with that of other methods, such as a concentric cylinder method and a hot wire method.

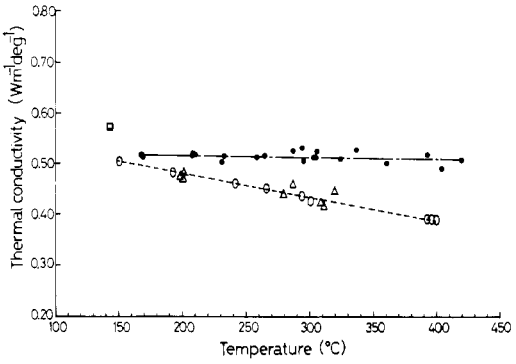

Figure 4. Thermal conductivity of HTS: - – ●, present work; - - ○ - - - -, Turnbull (*14*) (a hot wire method); △, Cooke (*3*) (a variable gap method); □, Gambill (*4*).

The time of onset of convective motion t_c is expressed by (*5*)

$$t_c = \sqrt{R_a \eta C_p / \pi g \alpha Q} \qquad (5)$$

When convection starts to take place, a plot of X_i^2 vs. t deviates from a straight line. From the analysis of a plot of X_i^2 vs. t in the experiments of distilled water, the value of R_a is estimated for this apparatus from eq 5 to be about 900. With this value and Q (~0.3 W cm^{-2}), t_c at 350 °C for $NaNO_3$ is calculated to be about 10.5 s, which is about 2 s longer than the experimental finding. At about 400 °C, the calculated t_c is even longer than the experimentally determined value (4.5 s).

As the temperature of the bulk liquid rises, the linear part of a plot X_i^2 against t becomes shorter and therefore the value $X_i/\sqrt{t}$ calculated from the linear part is expected to become less reliable.

In the case of $NaNO_3$, however, this is not a serious problem at least at 400 °C, where the standard deviations of the slopes of the linear parts are less than 0.5% in the least-squares fits.

In connection with experiments using the hot wire method, White (*17*) pointed out the possibility of electric current leaking through the testing liquid. This phenomena should be negligible in the present case, since the fringes are parallel to the heating foil before the onset of convection, and the calculated diffusivity or conductivity is not high in comparison with those measured by others, as seen from Figure 3. Figure 3 indicates that the thermal conductivities calculated from our thermal diffusivity data by eq 2 and 3 are in good agreement in the case of molten $NaNO_3$. Thus, for the calculation of thermal conductivity from thermal diffusivity, it is more convenient and probably more reliable to employ the relation of eq 3 than of eq 2, since C_p and ρ can be measured accurately to at least three significant digits, whereas the measurement of $(\partial n/\partial T)$ is rather troublesome.

A method of directly measuring the thermal diffusivity of molten salts has been proposed by Kato et al. (*9*), and our results on the thermal diffusivity of $NaNO_3$ are in good agreement with theirs, although the precision of their results is not so good as that of the results reported in this paper.

As seen from Figure 3, the thermal conductivity determined for molten $NaNO_3$ in the present experiment is consistent with those determined by others; however, in the present experiment and in the hot wire experiment by McLaughlin (*12*) it is almost independent of temperature, while in other experiments it increases slightly with temperature.

In the case of experiments using mixtures such as HTS, the present method has the advantage that a check on the uniformity of interferograms before charging the foil with electric current can confirm complete mixing of the salts. Table III shows that in the present study the thermal diffusivity of HTS increases slightly with temperature. Applying the least-squares method

Table III. Experimental Data for HTS

Temp (°C)	Thermal diffusivity $\times 10^7$ (m^2 s^{-1})	Thermal conductivity[a] (W m^{-1} deg^{-1})
167	1.69	0.517
168	1.68	0.514
208	1.69	0.509
208	1.73	0.521
212	1.71	0.514
231	1.67	0.499
232	1.72	0.514
257	1.73	0.512
263	1.76	0.519
286	1.80	0.526
293	1.82	0.531
294	1.72	0.501
302	1.77	0.514
304	1.76	0.511
305	1.80	0.523
324	1.76	0.507
336	1.84	0.528
360	1.75	0.497
391	1.84	0.516
403	1.75	0.488
419	1.81	0.502

[a] Calculated with C_p = 0.373 cal g^{-1} deg^{-1} and $\rho = 1.98 - 7.29 \times 10^{-4}$ $(T - 142)$ g cm^{-3} (*10*).

to the values for the thermal conductivity calculated from eq 3 combined with eq 1, we have found that the thermal conductivity is expressed as a function of temperature by

$$K = 0.519 - 4.7 \times 10^{-5}(T - 142)$$

This equation shows that the thermal conductivity of HTS is practically independent of temperature, which is in contrast with the findings by Turnbull (*14*) and Cooke (*3*), that the thermal conductivity decreases with increasing temperature, the temperature coefficient being about -5×10^{-4} W m^{-1} deg^{-2}.

According to Bloom (*1*) and McDonald (*11*), the temperature dependence of the thermal conductivity of a molten mixture of $NaNO_3$–KNO_3 is much the same as that of the single salts. The thermal conductivity of $NaNO_2$ has been reported by Bloom (*1*) to increase slightly with increasing temperature. Therefore, it would seem reasonable that the thermal conductivity of HTS is almost independent of temperature, as the present observation shows.

Glossary

K	thermal conductivity, W m^{-1} deg^{-1}
κ	thermal diffusivity, m^2 s^{-1}
T	temperature, °C
X	distance between a pair of fringes
t	time, s
b	shear produced by the beam splitter of the interferometer
Q	heat liberated at the foil, W m^{-2}
d	half width of the heating foil
λ	wavelength of the light, nm
n	refractive index
C_p	specific heat, W g^{-1} deg^{-1}
ρ	density, g m^{-3}
R_a	Rayleigh number
η	viscosity
g	acceleration of gravity
α	thermal expansivity
ΔR	optical path difference
l	geometric length of the light path through the liquid

Literature Cited

(1) Bloom, H., Doroszkowski, A. A., Tricklebank, S. B., *Aust. J. Chem.*, **18**, 1171 (1965).
(2) Bryngdahl, O., *Ark. Fys.*, **21**, 289 (1962).
(3) Cooke, J. W., ORNL-4831 (1973).
(4) Gambill, W. R., *Chem. Eng.*, **66**, 129 (1959).
(5) Gustafsson, S. E., *Z. Naturforsch. A*, **22**, 1005 (1967).
(6) Gustafsson, S. E., Halling, N.-O., Kjellander, R. A. E., *Z. Naturforsch. A*, **23**, 44 (1968).
(7) Gustafsson, S. E., Karawacki, E., *Appl. Opt.*, **14**, 1105 (1975).
(8) Janz, G. J., "Molten Salt Handbook", Academic Press, New York, N.Y., 1967, pp 42, 200.
(9) Kato, Y., Kobayasi, K., Araki, N., Furukawa, K., *J. Phys. E*, **8**, 461 (1975).
(10) Kirst, W. E., Nagle, W. M., Castner, J. B., *Trans. Am. Inst. Chem. Eng.*, **36**, 371 (1940).
(11) McDonald, J., Ph.D. Thesis, University of Minnesota, 1969.
(12) McLaughlin, E., *Chem. Rev.*, **64**, 389 (1964).
(13) Touloukian, Y. S., "Thermophysical Properties of Matter" (TPRC Data Series) Vol. 10, IFI/Plenum Data Corp., New York, N.Y., 1971.
(14) Turnbull, A. G., *Aust. J. Appl. Sci.*, **12**, 30 (1961).
(15) Uhl, V. W., Voznick, H. P., *Chem. Eng. Prog.*, **59**, 33 (1963).
(16) Wendelöv, L. W., Gustafsson, S. E., Halling, N.-O., Kjellander, R. A. E., *Z. Naturforsch. A*, **22**, 1363 (1967).
(17) White, L. R., Davis, H. T., *J. Chem. Phys.*, **47**, 5433 (1967).

Received for review August 17, 1976. Accepted December 16, 1976.

Apparent Molar Volumes of Some Complex Cyanides in Aqueous Solutions at 15–60 °C

Geoffrey Curthoys and John G. Mathieson†*
Department of Chemistry, University of Newcastle, N.S.W., 2308, Australia

The apparent molar volumes (ϕ_V) of a series of six complex cyanide compounds have been measured in aqueous solutions in the concentration range 0.001–0.5 mol dm^{-3}, and at five temperatures in the range 15–60 °C. The compounds studied are $K[Ag(CN)_2]$, $K_2[Ni(CN)_4]$, $K_3[Co(CN)_6]$, $K_3[Fe(CN)_6]$, $K_4[Fe(CN)_6]$, and $K_4[Mo(CN)_8]$. At higher concentrations ($c > 0.05$ mol dm^{-3}) ϕ_V was determined directly from pycnometer density measurements, while in the lower concentration region the dilatometer technique of Hepler, Stokes, and Stokes was employed.

The apparent molar volumes (ϕ_V) of many simple salts and salts containing large hydrophobic ions have been accurately measured in aqueous solutions (cf. the extensive compilation of Millero (*12*)). Few data, however, are available for the molar volumes of large hydrophilic ions or complex ions. Therefore we have measured apparent molar volumes as part of an extended study (*9, 10*) of the thermodynamic and transport properties of aqueous solutions of some complex cyanide compounds. In this paper we report ϕ_V measurements for $K[Ag(CN)_2]$, $K_2[Ni(CN)_4]$, $K_3[Co(CN)_6]$, $K_3[Fe(CN)_6]$, $K_4[Fe(CN)_6]$, and $K_4[Mo(CN)_8]$. Studies were made at 15, 25, 35, 45, and 60 °C using pycnometric density determinations, accurate to $\pm 1 \times 10^{-5}$ g cm^{-3}, for solutions of concentration $0.5 > c > 0.05$ mol dm^{-3}. For solutions of lower concentration pycnometry does not yield sufficiently accurate ϕ_V values (see below) and the dilatometer technique of Hepler, Stokes, and Stokes (*6*) was employed in the concentration region $0.001 < c < 0.05$ mol dm^{-1}. Infinite dilution values of ϕ_V (i.e., ϕ_V^0) have been determined by an extrapolation procedure which assumes Debye–Hückel limiting law behavior at low concentrations.

Experimental Section

Density measurements were made according to recommended methods (*15*) using two Sprengel-Ostwald pycnometers of approximately 30-cm^3 capacity with arms made of capillary tubing of 0.3 mm internal diameter. Before weighing, the filled pycnometers were equilibrated for about an hour in a large (600 L) efficiently stirred, insulated bath, whose temperature was controlled to $\pm 5 \times 10^{-4}$ °C or better by a mercury–toluene regulator operating a 60-W light bulb as the on–off heater. Buoyancy corrections were made and duplicate measurements agreed to $\pm 1 \times 10^{-5}$ g cm^{-3}. The bath temperature was calibrated against standardized mercury in glass thermometers. This bath was also used for the dilatometer measurements.

Dilatometer measurement techniques essentially similar to those described by Hepler, Stokes, and Stokes (*6*) were employed in this study. Dilatometers from 300 cm^3 to 1 dm^3 with capillaries of 1.00 mm diameter and with capsules from 3 to 60 cm^3 provided an adequate range of final concentrations. The measurement consists of observing the change in height (corrected for hydrostatic head) of solution in the capillary (Δh(corr)) as concentrated solution in the capsule, of known ϕ_V from density measurement, is mixed with pure solvent in the dilatometer flask. Since the capillary diameter is known Δh(corr) can be directly related to the volume change on dilution, Δv.

Calculations and Errors

The apparent molar volume of a solute in a solution of density d, g cm^{-3}, is given by,

$$\phi_V = \bar{M}_2/d_0 - 1000(d - d_0)/cd_0 \ldots \quad (1)$$

where $\bar{M}_2$ is the molecular weight of the solute, d_0 is the solvent density, and c is the solute concentration in mol dm^{-3}. Errors in the concentration of carefully prepared solutions do not affect ϕ_V significantly; however, differentiation of eq 1 at constant concentration gives,

$$\delta\phi_V = \left| \frac{1000}{c} \frac{\delta d}{d} \right| \quad (2)$$

Thus for a given uncertainty in density, the uncertainty in ϕ_V is inversely proportional to concentration. Using an uncertainty in density appropriate for our pycnometers, i.e., $\delta d/d = 2 \times 10^{-5}$ $\delta\phi_V$ is already 0.2 cm^3 mol^{-1} at 0.1 mol dm^{-3} and increases rapidly at lower concentrations.

In dilatometer experiments the apparent molar volume of the final dilute solution ϕ_V^{final} is related to that of the initial concentrated solution, ϕ_V^{init} (determined by density measurement)

† Department of Chemistry, Monash University, Wellington Road, Clayton, Victoria, 3168, Australia.